RSC Advances

ROYAL SOCIETY OF CHEMISTRY

www.rsc.org/advances

Laser Irradiation Induced Photo-crystallization in Nano-Structured Amorphous $Se_{90-x}Hg_xS_{10}$ (x = 0, 5, 10, 15) Thin Films

Shabir Ahmad[a], K. Asokan[b], M. Zulfequar[a]*.

[a]Department of Physics, Jamia Millia Islamia, New Delhi-110025, India
[b]Materials Science Division, Inter University Accelerator Centre, New Delhi-110067, India
*Corresponding author. Email: mzulfe@rediffmail.com

Abstract

Present study focuses on the influence of laser irradiation induced photo crystallization and the modification in the optical and electrical properties of thermally evaporated amorphous $Se_{90-x}Hg_xS_{10}$ (x = 0, 5, 10, 15) thin films. The chemical composition and amorphous nature of the as-prepared thin films were examined by energy dispersive X-ray analysis and X-ray diffraction (XRD) respectively. However, the XRD analysis revealed the crystalline nature of thin films irradiated by 337.1 nm pulsed laser. These results are further investigated by surface morphological techniques using Atomic force microscopy (AFM) and Scanning electron microscopy (SEM). An enhancement in average grain sizes after laser irradiation was observed. From absorption spectra by UV-vis-spectrophotometer were evaluated using the Urbach's edge method. As the duration of laser irradiation increased, the optical energy gap and tail energy width for all these compositions decreased. Further, it has been observed that the value of optical energy gap decreases with Hg content in the Se-S alloy. These results have been interpreted on the basis of laser irradiation-induced photo-crystallization in the film. Electrical analysis such as dark dc conductivity and photoconductivity in the temperature range 310-390 K show enhancement of the electrical conductivity and the reduction of activation energy as the irradiation time increases and specifies that the density of defect states decreases after irradiation. Temperature dependent photoconductivity measurements show similar trends as that of dark conductivity. This is because, the photo-created carriers can move easily in laser irradiated thin films due to the crystallinity of the material.

Keywords: Thin films; Laser-irradiation; Optical band gap; d.c. conductivity; Photosensitivity.

1. Introduction

Metal based chalcogenides possess most desirable physical properties especially optical for potential applications. A major advantage of chalcogenide semiconductor thin films is the controlled response to external stimuli such as heat treatment, laser irradiation, gamma irradiation, swift heavy ion irradiation etc. which makes them feasible for several advanced applications like optical computing, optical data storage, ultrafast optical switches, optical sensors etc. [1-4]. During the process of light-matter interaction, electrons and holes are created; these photo-created carriers may not remain free but can become trapped, or localized in one way or another in the band tail states of amorphous semiconductors. Such localized states exhibit a strong electron-phonon coupling which may lead a structural rearrangement of the 'lattice', and hence changes in the physical properties causing photo-darkening, photo-expansion, photo-crystallization, etc. [5-8]. The knowledge of the optical and electrical properties of these chalcogenide glasses is obviously necessary for exploiting their very interesting technological applications. However, due to their outstanding performance in the technological field, various investigations have been reported so far regarding the study of optical properties of chalcogenide thin films [9-12]. Optical absorption data provide the information on the band structure and the energy gap of semiconductors and hence understanding and developing the energy band diagram is possible for both crystalline and amorphous materials.

In the present study, the influence of pulsed laser irradiation on structural, optical and electrical parameters of $Se_{90-x}Hg_xS_{10}$ (x = 0, 5, 10, 15) thin films have been investigated by analyzing the absorption spectra in the spectral range of 400 -800 nm for optical study and the temperature range 310-390 K for electrical study. We have used Selenium (Se) as a major content as it has wide commercial applications in many industrial fields, such as Xerography, photo rectifiers, solar cells [13-15], photoconductor for high-definition television (HDTV) [13], digital radiography (DDR) [16] etc. This is because of high spatial resolution, low thermal noise and high sensitivity against wide variety of wavelengths from visible to ultraviolet [17] as well as x-rays [18, 19] as compared to Si based photoconductors. But pure Se has many disadvantages like low sensitivity and short lifetime. To overcome these disadvantages, we have selected Hg as an additive element with Se. As it is an only metal, except rubidium, gallium and cesium, that could be in liquid state near room temperature, this makes it possible to be used as high temperature thermometer. There is a strong tendency for Hg to supercool below its freezing point, so, seeding may be necessary to initiate solidification. The addition of third element sulphur (S) enhances the electrical conductivity as evident from various studies for similar type of alloys [20, 21].

2. Experimental Studies

The bulk samples of $Se_{90-x}Hg_xS_{10}$ (x = 0, 5, 10, 15) ternary chalcogenide glass were prepared from stoichiometric mixture of highly pure (99.999% purity) Se, S and Hg. The constituent elements were weighed in accordance with their atomic percentages using an electronic balance having the least count of 10^{-4} gm. The material was then sealed in chemically cleaned and evacuated (~10^{-5} torr) quartz ampoules (length ~ 5cm and internal diameter ~ 8mm). The sealed ampoules were placed in a Microprocessor-Controlled Programmable Muffle Furnace, where the

temperature was increased at a constant heating rate of 4 °C/min up to 900 °C and the material within the ampoules is allowed to melt at 900 °C for 15 h. During heating, the ampoules were constantly rocked, by rotating a ceramic rod to which the ampoules were tucked away in the furnace in order to obtain homogeneous glassy alloy. After rocking for about 15 hours, the obtained melt was rapidly quenched in ice-cooled water. After quenching, ingot has been removed by breaking the ampoules and grinded into a fine powder with the help of pestle and mortar. From this powder, thin films were deposited by thermal evaporation technique on cleaned glass substrates, at room temperature under a pressure of ~10^{-5} torr through molybdenum boat. The glass substrates were first cleaned in ultrasonic bath and then by acetone. For achieving meta-stable equilibrium, the films were kept inside the deposition chamber for 24hrs as suggested by Abkowitz [22]. The radiation treatment of these thin films was performed by TEA N_2 pulsed laser having wavelength 337.1 nm, power 100 kW and pulse width 1 ns, for different durations of time, 5, 10, and 15 min. The elemental composition of the investigated thin films was verified by energy dispersive x-ray (EDX) technique. A Rigaku Ultima IV X-ray diffractometer (XRD) was carried out in the scanning angle range of 10^o- 60^o for studying the structure of as-prepared and laser-irradiated thin films. The copper target (Cu $K\alpha_1$) was used as X-rays source with λ= 1.54560Å. The surface morphology of investigated thin films was studied by using Field Emission scanning electron microscope (FESEM) (Model: Σigma by Carl Zeiss employed with Gemini Column (Patented technology of Corl Zeiss). The surface morphology of these films was analyzed by Atomic Force Microscopy (AFM) (Nanoscope IIIa) in tapping mode in which the images were recorded before and after irradiation. The optical characterization of thin films were carried out by using VU-vis-spectrophotometer (Model: Camspec M550 double beam) in the wavelength range 400-800nm. An electrode with 1 mm gap was made by using the silver paste on the thin films. Dark dC conductivity and photoconductivity measurements were carried out in the temperature range of 310-390 K at constant voltage of 1.5 V by mounting the thin films in a specially designed metallic sample holder in which white light (200W tungsten lamp) shown through a transparent window. The thermal effects produced due to lamp are not predominating because of its negligibly small temperature (nearly 2-4 K). The intensity of the lamp was measured to be 3650 lx by a digital Luxmeter (MS6610).

3. Results

3.1. X-ray diffraction (XRD) Studies

X-ray diffractometer (XRD) was employed for studying the structure of as-prepared and irradiated thin films of $Se_{90-x}Hg_xS_{10}$ (x = 0, 5, 10, 15). The X-ray diffraction patterns were obtained at room temperature, illustrated in Fig.1. The absence of any sharp structural peaks in the XRD patterns of as-prepared thin films confirms the amorphous nature while the presence of sharp structural peaks in the XRD patterns of 15 min laser-irradiated thin films could be indicative of irradiation induced crystallization due to grain growth. Thus XRD analysis clearly revealed the amorphous to crystalline phase transition after laser irradiation. Similar results were

also reported by other workers for different chalcogenide glasses [23, 24]. The peak values of laser–irradiated thin films matches well with cubic structure as per the standard data file (Card no. 22-0729). The crystallite size of 15 min laser irradiated thin films of $Se_{90-x}Hg_xS_{10}$ (x = 0, 5, 10 and 15) were calculated at the prominent (111) peak by using Scherrer's formula [25].

$$D = \frac{0.94\lambda}{\beta \cos\theta} \quad (1)$$

Where 'D' is the crystallite size, 'λ' is the wavelength of the X-ray used (i.e., λ= 1.54560 Å), 'β' is the full-width at half-maximum (FWHM) and 'θ' is the Bragg's angle of reflection. The calculated grain size values are 69.23 nm, 78.52 nm, 82.01 nm and 100.22 nm for 15 min laser irradiated thin films of $Se_{90-x}Hg_xS_{10}$ (x = 0, 5, 10 and 15) respectively.

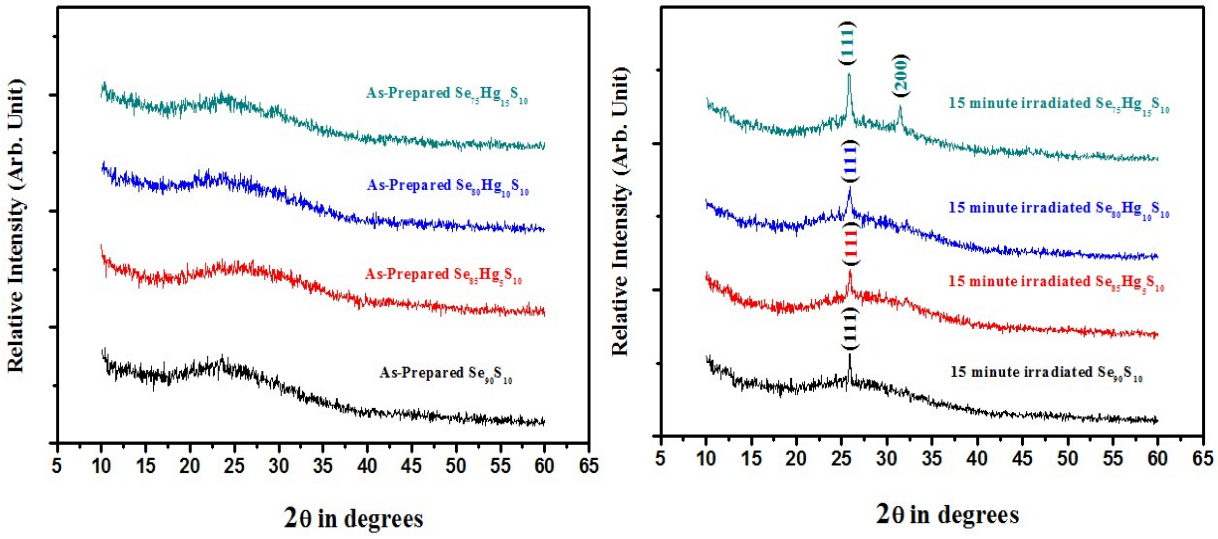

Figure.1. XRD patterns of (a) as-prepared and (b) 15 minute laser irradiated thin films of $Se_{90-x}Hg_xS_{10}$ (x = 0, 5, 10, 15).

3.2 Elemental composition and Surface Morphological analysis

The elemental composition analysis was carried out by EDX technique. Fig.2. shows the typical EDX patterns of as-prepared thin films of$Se_{90-x}Hg_xS_{10}$ (x = 0, 15). The calculated wt% shows Se (89.82%), S (10.12%) for $Se_{90}S_{10}$ and (74.12%), S (9.64%),Hg (16.24%) for $Se_{90}Hg_{15}S_{10}$. Similaly the wt% of other compositions agrees well with expermentally taken wt%. An intense peak for Se was found in the spectra is due to its high concentration as in comparision to S and Hg. The wt% of the C, Si, Na and Ca that arises due to glass substrates are omitted in the analysis.

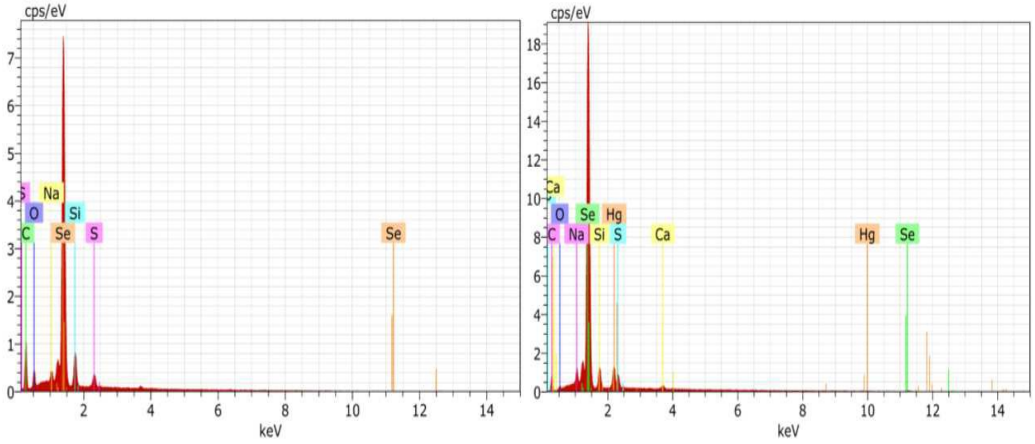

(a) (b)

Figure.2. EDX spectra of as-prepared thin films of (a) $Se_{90}S_{10,}$ and (b) $Se_{90}Hg_{15}S_{10}$.

Surface Morphological Analysis

SEM is the suitable technique to study the microstructure of the thin films. Fig.3. shows a typical SEM images of as-prepared and 15 min laser irradiated thin films of $Se_{90-x}Hg_xS_{10}$ (x = 0, 15). It is clear from these images, that the laser irradiated thin films show crystallites with developed facets which are due to laser pulses. This is because irradiation initiates nucleation and grain growth. The grain size as calculated from SEM images of these films varies from 36 to 62 nm for $Se_{90}S_{10}$ and 59 to 98 nm for $Se_{90}Hg_{15}S_{10}$. Similar trend was also found in other compositions (Fig not shown).

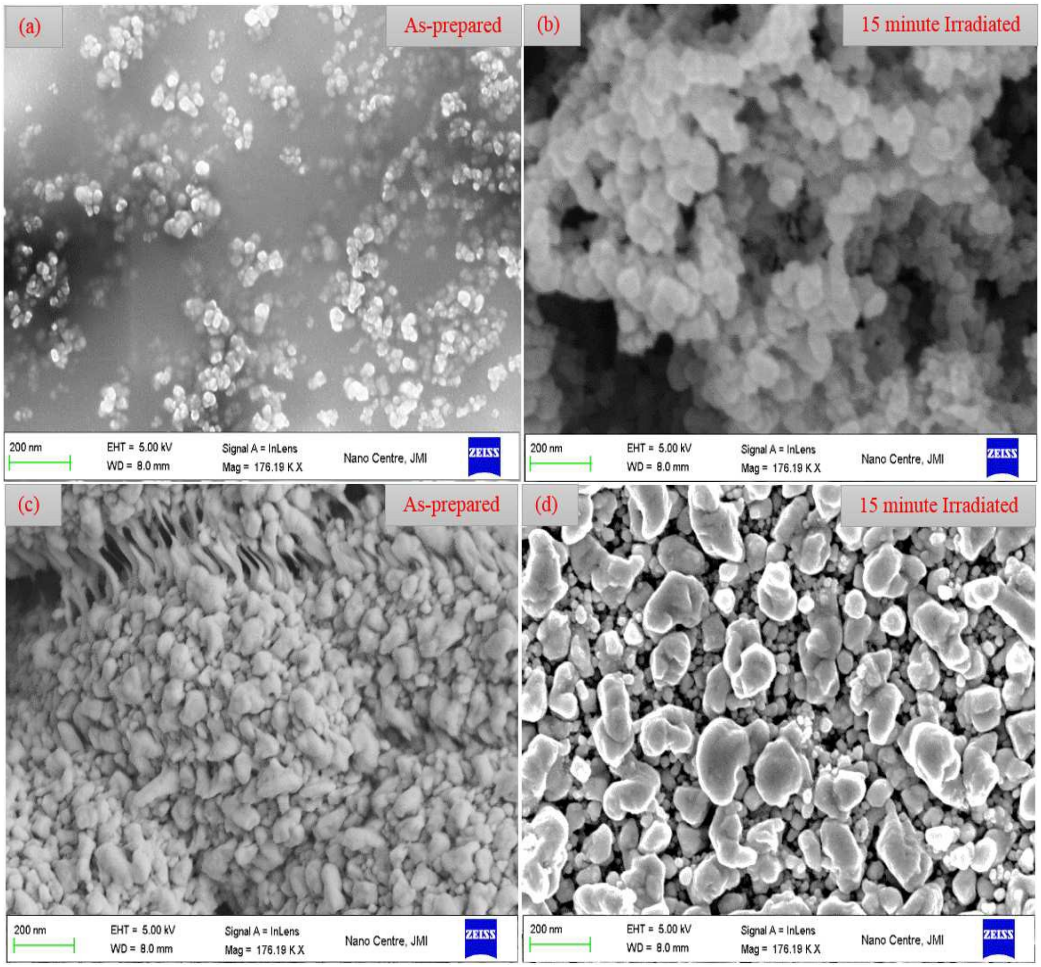

Figure.3. SEM images of (a, c) as-prepared and (b, d) 15 minute laser irradiated thin films of $Se_{90-x}Hg_xS_{10}$ (x = 0, 15).

The typical two-dimensional and three-dimensional (2D and 3D) AFM images are depicted in Fig.4 for the $Se_{90-x}Hg_xS_{10}$ films with Hg content x = 0 and 15 respectively. It is observed that the grain size increases with laser irradiation. The calculated grain size values of as-prepared thin films of $Se_{90-x}Hg_xS_{10}$ (x = 0, 5, 10, 15) are 37 nm, 43 nm, 50 nm and 58 nm respectively whereas for irradiated thin films, the grain size values are 59 nm, 71 nm, 83 nm and 95 nm repectively for same composition. The calculation of average surface roughness (Ra) values for these as-prepared thin films show very low values 0.11, 0.12, 0. 12, and 0.10 nm respectively for $Se_{90-x}Hg_xS_{10}$ (x = 0, 5, 10, 15). Such very low values predict the uniform surface of the $Se_{90-x}Hg_xS_{10}$ films when prepared by the thermal evaporation technique. It shows the compactness, pin hole free and well adhesive nature of these films on glass substrates which will be very much useful for various optoelectronic devices. After irradiation the average surface roughness (Ra) values of $Se_{90-x}Hg_xS_{10}$ (x = 0, 5, 10, 15) decreases to 0.09, 0.09, 0.10 and 0.08 nm, respectively. These AFM images confirm the previous results obtained from SEM and XRD analysis of $Ga_{10}Se_{85}Hg_5$.The AFM analysis shows the grain size increases with addition of Hg in the Se-S alloy. This is expected because the atomic radius of Hg is 0.151 nm, which is greater than the

atomic radius of Se 0.117 nm. Present study of $Se_{90-x}Hg_xS_{10}$ films makes a very good solid solution which means that Hg replaces Se atoms in the crystal lattice. This leads to the formation of linear grains with an enhancement of grain size when one mixes to Se-S with various amounts of Hg-Se.

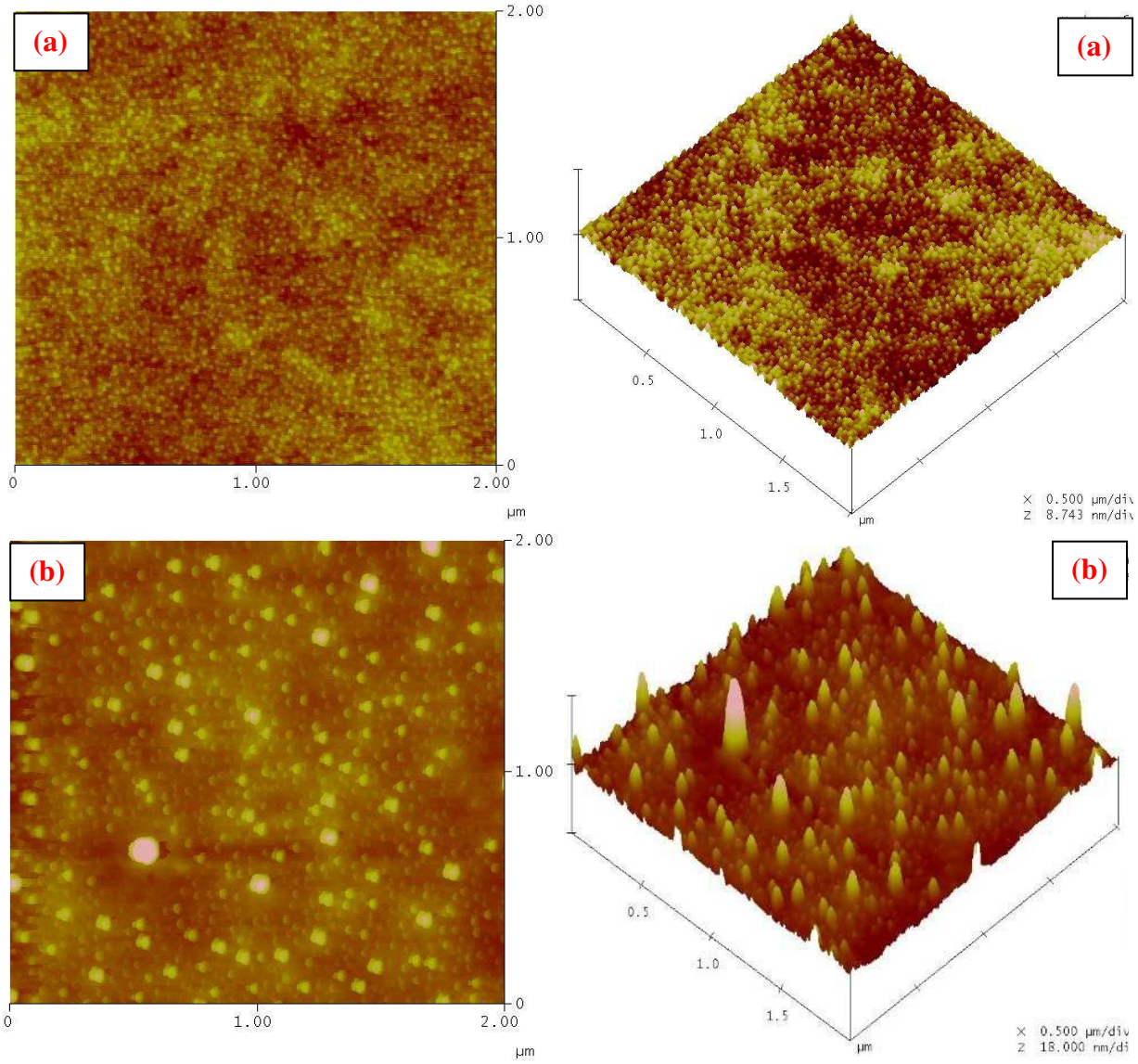

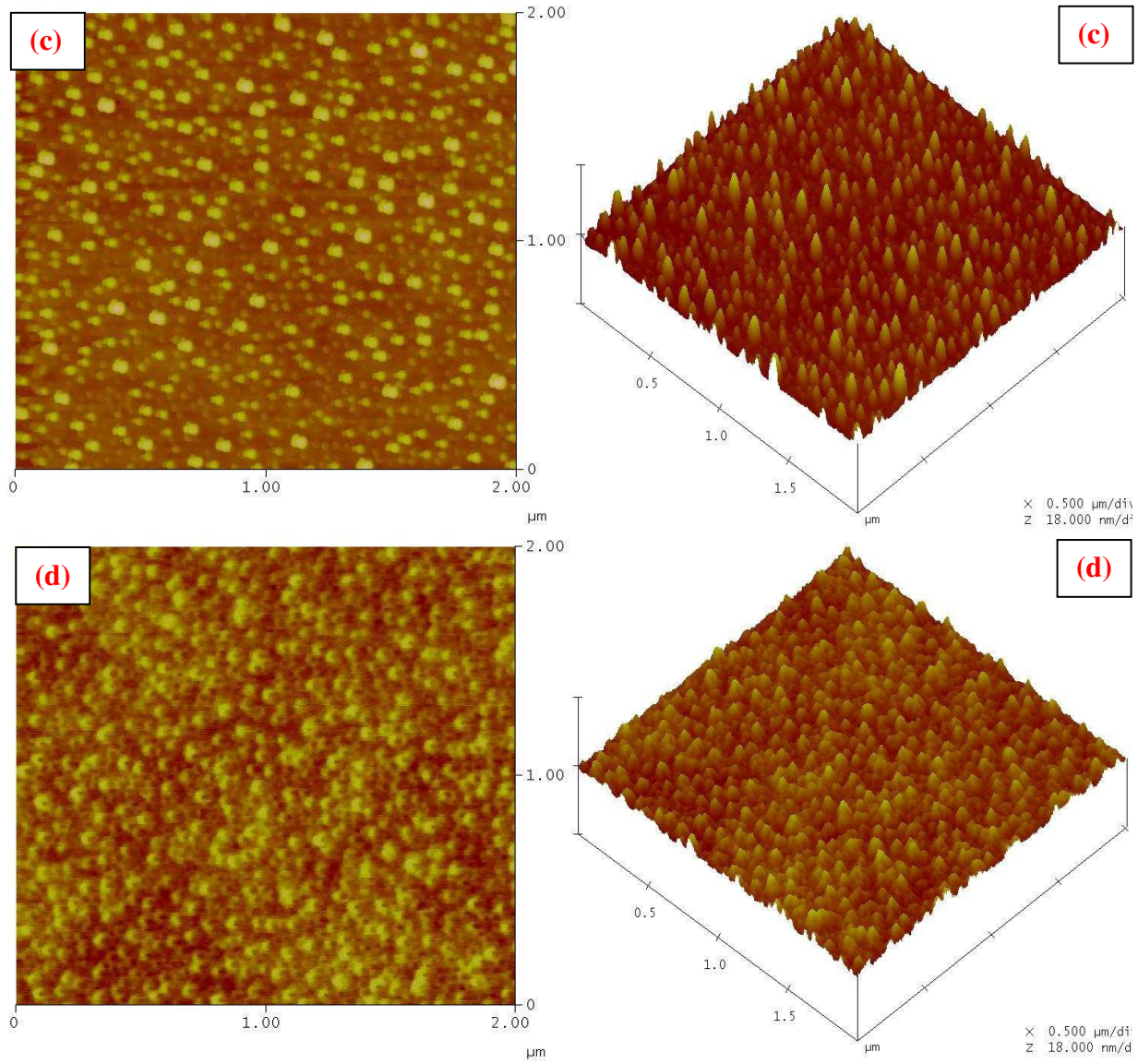

Figure.4. AFM images (2 dimensional and 3 dimensional) of (a, b) as-prepared and (c, d) 15 minute laser irradiated, thin films of $Se_{90-x}Hg_xS_{10}$ (x = 0, 15).

3.3. Optical Studies

The optical absorption of the investigated thin films was measured in the wavelength range 400-800 nm as shown in Fig.5. This is used to determine its optical constants like absorption coefficient (a), extinction coefficient (k), optical band gap (E_g), Urbach's energy (E_u) etc.This is because optical absorption spectrum is one of the most dynamic, simple and yet most useful optical technique for explaining various features concerning the band structure and the energy gap of amorphous materials.

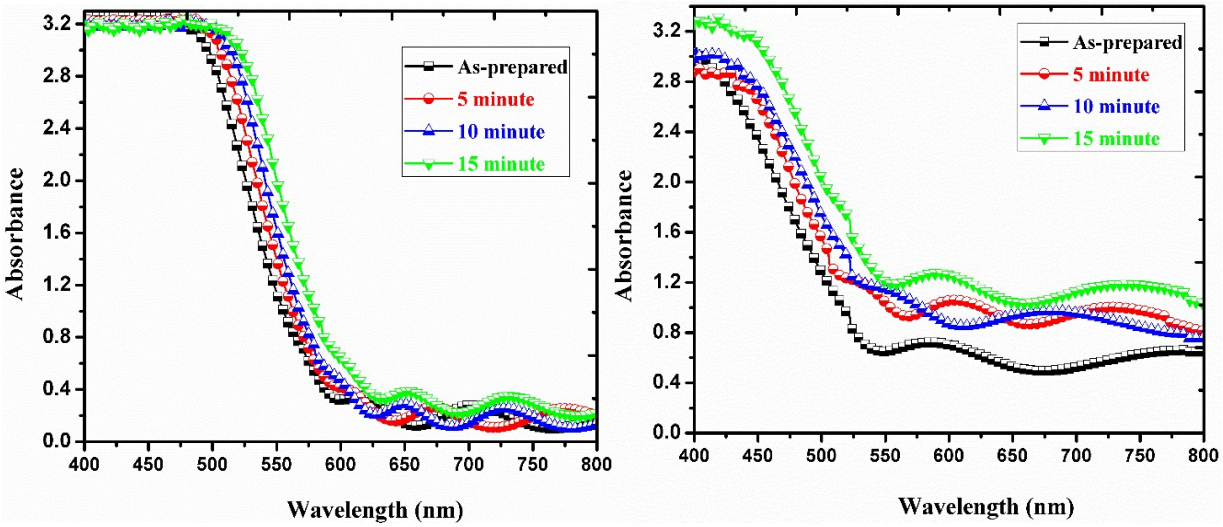

Figure.5. Optical absorption spectra of as-prepared and laser irradiated thin films of (a) $Se_{90}S_{10,}$ and (b) $Se_{75}Hg_{15}S_{10}$.

The absorption coefficient (α) is calculated directly from the absorbance vs wavelength curves using the relation [26, 27]

$$\alpha = \frac{\text{Absorbance}}{\text{Film thickness}} \qquad (2)$$

Fig.6. displays the typical UV–visible absorption coefficient spectra of as-prepared and laser irradiated (at 5, 10 and 15 min) $Se_{90-x}Hg_xS_{10}$ (0, 15) thin films measured at room temperature. The value of absorption coefficient (α) increases with the photon energy for as-prepared and laser irradiated thin films. In absorption process, a known energy of photon excites an electron from a lower to a higher energy state, corresponding to an absorption edge. In chalcogenide glasses, a typical absorption edge can be broadly ascribed to one of three processes: residual below-gap absorption, Urbach tails and inter-band absorption. Chalcogenide glasses have been found to exhibit highly reproducible optical edges which are relatively insensitive to preparation conditions and only the observable absorption [28] with a gap under equilibrium conditions account for the first process. In the second process the absorption edge depends exponentially on the photon energy according to the Urbach relation [29].

$$\alpha = \alpha_0 \exp(h\nu/E_u) \qquad (3)$$

Where α_0 is a constant, h is the plank's constant and E_u is the width of the band tail or Urbac's energy. The values of the Urbach's energy of the investigated thin films were estimated directly from the slopes of the plot ln(α) versus hν below the fundamental edge (not shown here). The calculated values of Urbach's energy decreases after laser irradiation, as illustrated in Table.1,

indicates the dense defect states are decreased in the forbidden gap leads to the crystallization of material after irradiation.

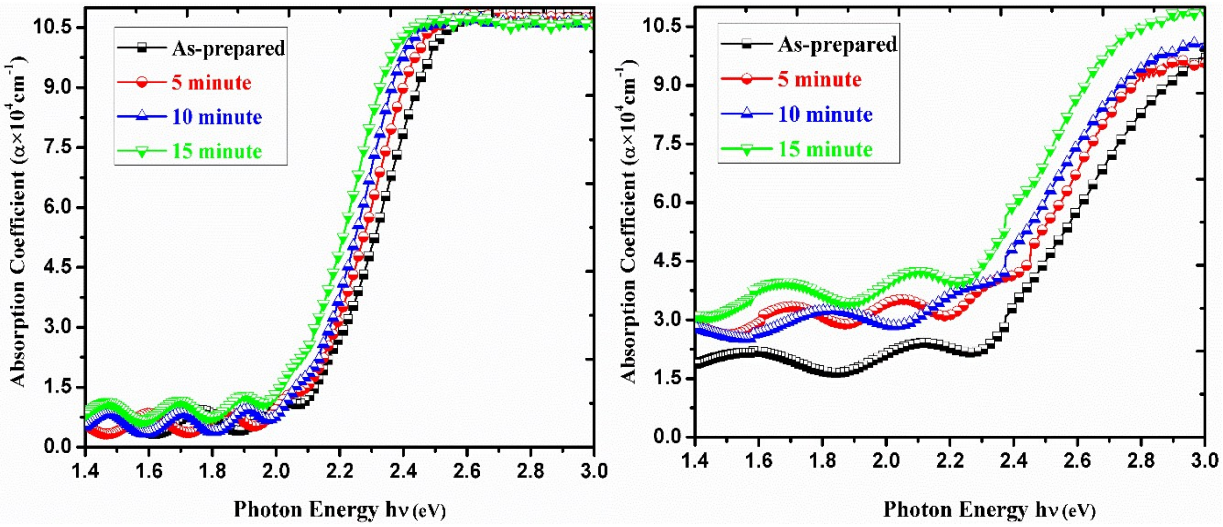

Figure.6. Variation of absorption coefficient (α) with incident photon energy of as-prepared and laser irradiated, thin films of (a) $Se_{90}S_{10}$, and (b) $Se_{75}Hg_{15}S_{10}$.

The optical band gap is determined by applying the Tauc model, [28] and the Davis and Mott model [30] in the high absorbance region

$$(\alpha h\nu) = B\,(h\nu - E_g)^n \qquad (4)$$

Where $(h\nu)$ is the photon energy, E_g is the optical band gap, and B is a constant. The exponent n is an index associated with the type of transition, which may be direct or indirect. Both types of transitions involve the interaction of electromagnetic waves (photons) with an electron in the valence band, which is excited across the gap to the conduction band. In fact n takes the values of 1/2 and 2 for allowed direct and indirect transitions respectively, and takes values of 1/3 and 3 for forbidden direct and forbidden indirect transitions. To obtain the value of n, several authors [31-33] have suggested that the quantity $(\alpha h\nu)^{1/n}$ must be plotted as a function of the incident photon energy (hν) for all possible values of n and the one which fits Eq.(4) will be taken as the value of n. In the present system, the value of n comes out to be 2 indicating that allowed indirect optical transitions are involved in the investigated thin films as shown in Fig.7. The calculated optical band gap values of these films are summarized in Table 1. The values of optical band gap (Eg) decrease continuously with increasing the exposure time of laser irradiation. Similar results were also reported for other amorphous Se based alloys [2, 24]. This decrease in the optical band gap with irradiation is understood in terms of inducing crystallization in semiconducting glasses. Laser irradiation provides sufficient energy to break weaker bonds thus introducing some translational degree of freedom to the system resulting in an increase in the heat capacity of the

system and decrease in the optical energy gap. Consequently, crystallization via nucleation and growth becomes possible and depends on the laser irradiation. The amount of crystalline phase increases with exposure time. In this way, the decrease in optical band gap is attributed to the amorphous to crystalline phase transformations.

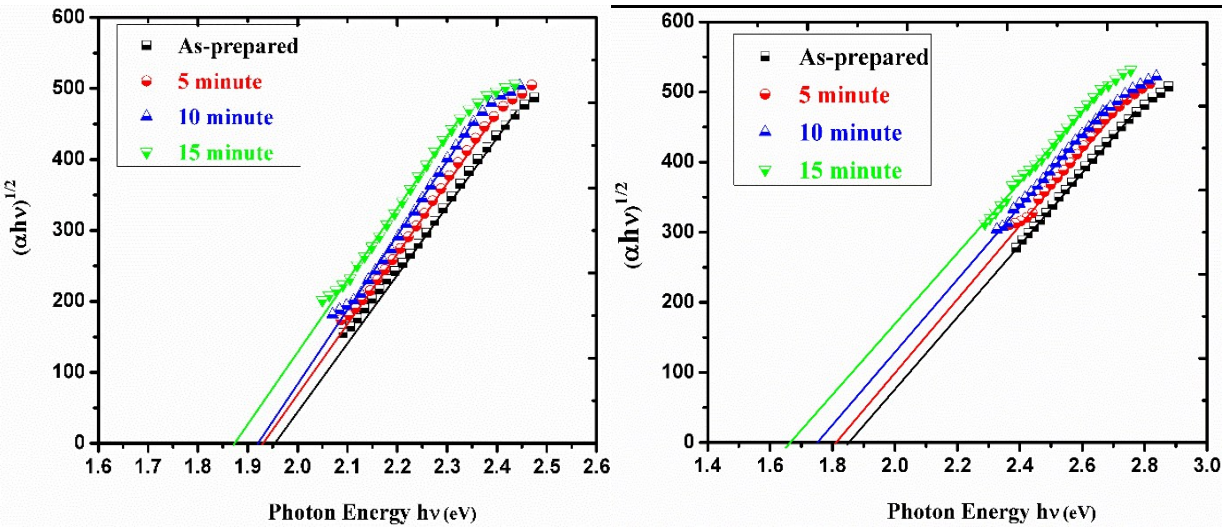

Figure.7. Variation of $(\alpha h\nu)^{1/2}$ with incident photon energy of as-prepared and laser irradiated, thin films of (a) $Se_{90}S_{10}$, and (b)$Se_{75}Hg_{15}S_{10}$.

Fig.8 shows the effect of grain size on band gap schematically. The homonuclear bond energies of S-S, Se-Se, Hg-Hg, and electro-negativities of S, Se, and Hg had been reported in various studies [20, 34]. The values of heteronuclear bond energies Se-S, Hg-Se, Se-Hg are calculated by using the values of electro-negativities and homonuclear bond energies in the equation reported in [20, 34]. This analysis shows the average bond energy decreases from 459.3 KJ/mol to 200.16 KJ/mol. Thus, it is expected that some homonuclear bonds break due to laser irradiation within the Se chain and new heteronuclear bonds are formed, because these require small energy for formation. In this process, the additive elements Hg and S can mix completely with Se. Hence, in this way the resultant particle size increases because the atomic radius of Hg is greater than the atomic radius of Se. Thus, according to the Young-Laplace equation [35], smaller the radius of the grain greater pressure is present and hence strong forces towards the interior of the grain. These abnormalities at the surface are responsible for changes of the inter-atomic forces and hence the band gap [36, 37].

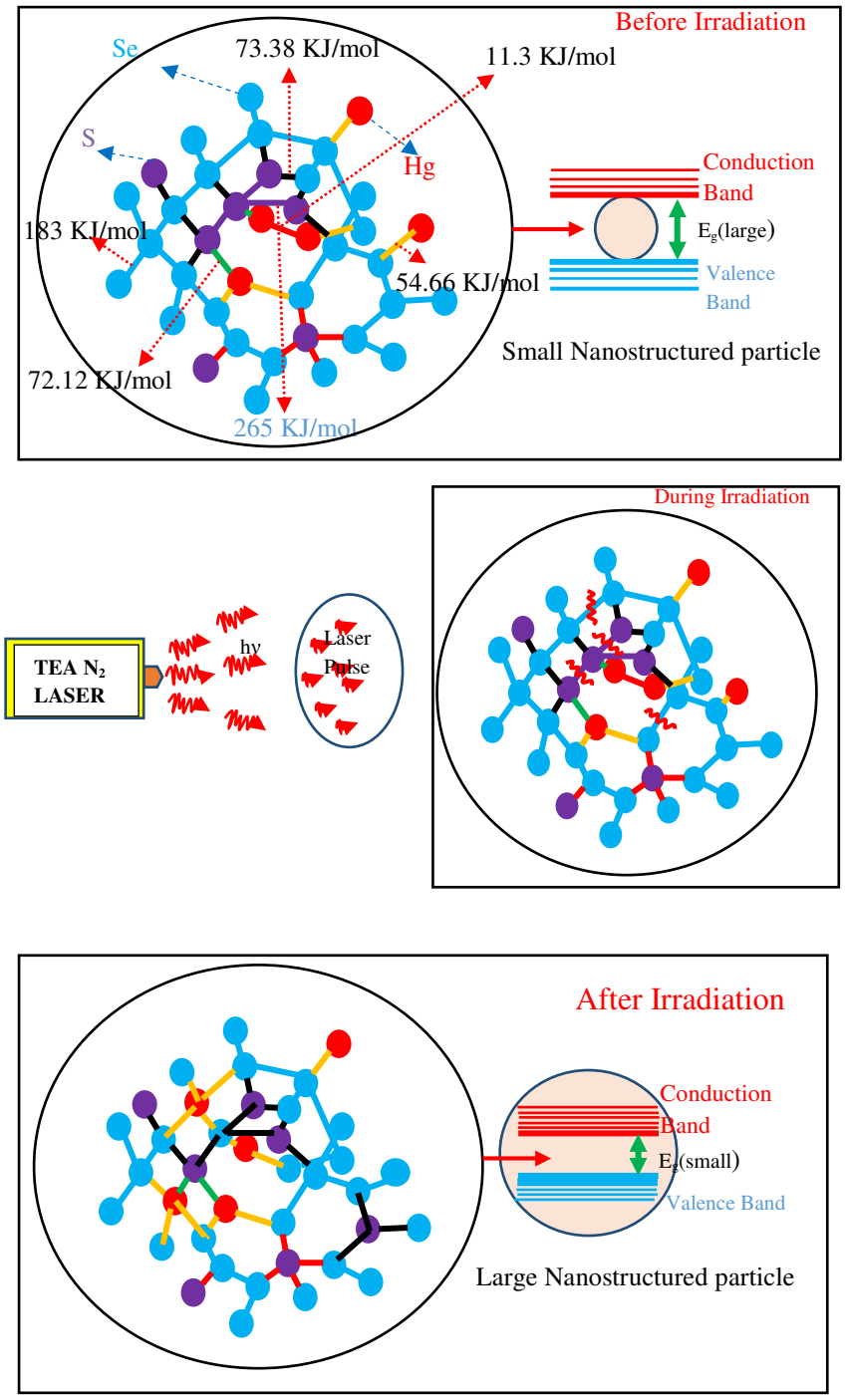

Figure. 8 shows the schematic representations of the effect of laser irradiations on grain size and band gap of Se-Hg-S thin films.

Table.1a. Optical parameters at a wavelength of 580 nm and electrical parameters at a temperature 341.29 K of as-prepared and laser irradiated thin films of $Se_{90}S_{10}$.

	Optical parameters				Electrical parameters				
Irradiation Time	E_g(eV)	$\alpha\times10^4$ (cm^{-1})	E_u(eV)	K	ΔE_{dc}(eV)	σ_{dc}($\Omega^{-1}cm^{-1}$)	σ_0($\Omega^{-1}cm^{-1}$)	ΔE_{ph}(eV)	σ_{ph}($\Omega^{-1}cm^{-1}$)
As-deposited	1.95± 0.001	1.749± 0.3	0.220	0.080	0.296	5.924×10^{-5}	1.392×10^{0}	0.328	2.221×10^{-5}
5 minute	1.92± 0.001	2.030± 0.3	0.218	0.093	0.290	6.664×10^{-5}	1.277×10^{0}	0.327	2.406×10^{-5}
10 minute	1.91± 0.001	2.268± 0.3	0.216	0.104	0.266	7.590×10^{-5}	6.433×10^{-1}	0.296	2.777×10^{-5}
15 minute	1.87± 0.001	3.338± 0.3	0.211	0.154	0.255	8.331×10^{-5}	4.857×10^{-1}	0.294	3.517×10^{-5}

Table.1b. Optical parameters at a wavelength of 580 nm and electrical parameters at a temperature 341.29 K of as-prepared and laser irradiated thin films of $Se_{95}Hg_5S_{10}$.

	Optical parameters				Electrical parameters				
Irradiation Time	E_g(eV)	$\alpha\times10^4$ (cm^{-1})	E_u(eV)	K	ΔE_{dc}(eV)	σ_{dc}($\Omega^{-1}cm^{-1}$)	σ_0($\Omega^{-1}cm^{-1}$)	ΔE_{ph}(eV)	σ_{ph}($\Omega^{-1}cm^{-1}$)
As-deposited	1.91± 0.001	1.641± 0.3	0.218	0.077	0.295	6.664×10^{-5}	1.514×10^{0}	0.253	2.591×10^{-5}
5 minute	1.88± 0.001	2.466± 0.3	0.216	0.115	0.293	7.590×10^{-5}	1.611×10^{0}	0.257	3.147×10^{-5}
10 minute	1.86± 0.001	2.524± 0.3	0.214	0.118	0.296	7.960×10^{-5}	1.871×10^{0}	0.253	3.517×10^{-5}
15 minute	1.85± 0.001	2.712± 0.3	0.212	0.126	0.250	8.516×10^{-5}	4.189×10^{-1}	0.242	6.109×10^{-5}

Table.1c. Optical parameters at a wavelength of 580 nm and electrical parameters at a temperature 341.29 K of as-prepared and laser irradiated thin films of $Se_{80}Hg_{10}S_{10}$.

	Optical parameters				Electrical parameters				
Irradiation Time	E_g(eV)	$\alpha\times10^4$ (cm^{-1})	E_u(eV)	K	ΔE_{dc}(eV)	σ_{dc}($\Omega^{-1}cm^{-1}$)	σ_0($\Omega^{-1}cm^{-1}$)	ΔE_{ph}(eV)	σ_{ph}($\Omega^{-1}cm^{-1}$)
As-deposited	1.90± 0.001	2.170± 0.3	0.215	0.100	0.282	7.775×10^{-5}	1.135×10^{0}	0.244	2.591×10^{-5}
5 minute	1.85± 0.001	2.876± 0.3	0.212	0.132	0.260	7.775×10^{-5}	5.374×10^{-1}	0.234	3.517×10^{-5}
10 minute	1.89± 0.001	2.244± 0.3	0.209	0.103	0.259	1.073×10^{-4}	7.173×10^{-1}	0.223	3.702×10^{-5}
15 minute	1.80± 0.001	3.739± 0.3	0.206	0.172	0.258	1.258×10^{-4}	8.129×10^{-1}	0.197	4.258×10^{-5}

Table.1d. Optical parameters at a wavelength of 580 nm and electrical parameters at a temperature 341.29 K of as-prepared and laser irradiated thin films of $Se_{75}Hg_{15}S_{10}$.

	Optical parameters				Electrical parameters				
Irradiation Time	E_g(eV)	$\alpha\times10^4$ (cm^{-1})	E_u(eV)	K	ΔE_{dc}(eV)	σ_{dc}($\Omega^{-1}cm^{-1}$)	σ_0($\Omega^{-1}cm^{-1}$)	ΔE_{ph}(eV)	σ_{ph}($\Omega^{-1}cm^{-1}$)
As-deposited	1.85± 0.001	2.398± 0.3	0.212	0.213	0.245	9.626×10^{-5}	3.995×10^{-1}	0.171	5.924×10^{-5}
5 minute	1.81± 0.001	3.245± 0.3	0.207	0.250	0.246	1.036×10^{-4}	3.815×10^{-1}	0.158	7.775×10^{-5}
10 minute	1.75± 0.001	3.291± 0.3	0.203	0.277	0.156	1.481×10^{-4}	2.981×10^{-2}	0.157	9.812×10^{-5}
15 minute	1.66± 0.001	4.197± 0.3	0.200	0.323	0.150	1.703×10^{-4}	2.795×10^{-2}	0.117	1.073×10^{-4}

The extinction coefficient (K) at different wavelength have been estimated by using the formula[27]

$$K = \frac{\alpha\lambda}{4\pi} \quad (5)$$

Where α and λ are the absorption coefficient and wave length of the incident photon respectively. The spectral dependence of extinction coefficient is shown in Fig.9. The values of extinction coefficient increase with the exposure time of irradiation as given in Table.1.

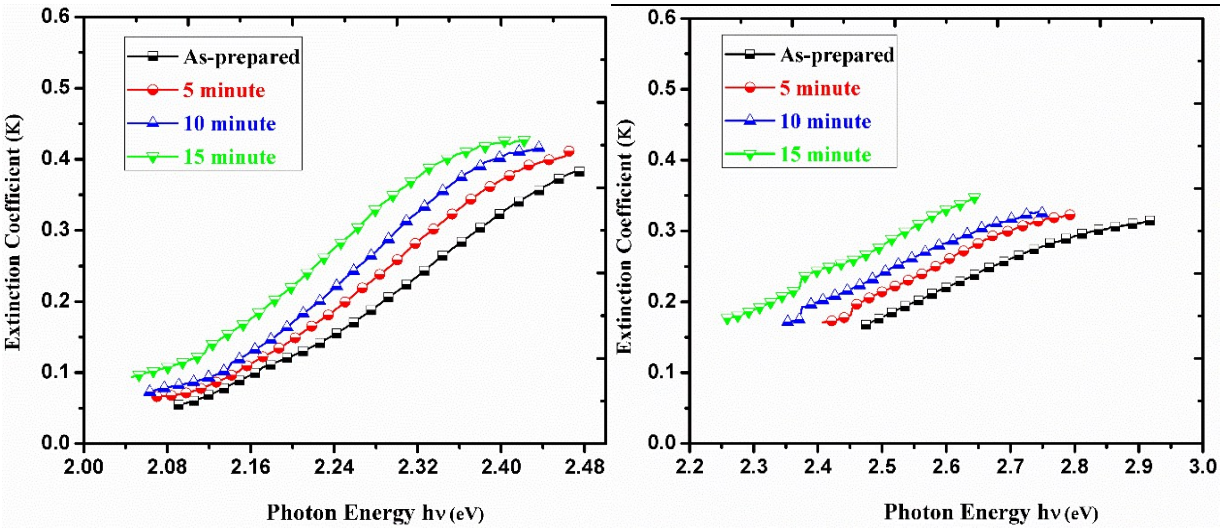

Figure.9. Variation of extinction coefficient (K) with incident photon energy of as-prepared and laser irradiated, thin films of (a) $Se_{90}S_{10}$, and (b) $Se_{75}Hg_{15}S_{10}$.

Electrical studies

The I_d-V and I_{ph}-V plots of $Se_{90-x}Hg_xS_{10}$ (x = 0,15) were measured at room temperature and are shown in Fig.10 and 11. These films display the ohmic behaviour and their both dark and photocurrent increase with the duration of laser irradiation. This change is found more in case of Hg doped Se-S alloy. Similar behaviours were also observed in $Se_{90-x}Hg_xS_{10}$ (x = 5, 10) (Fig. not shown).

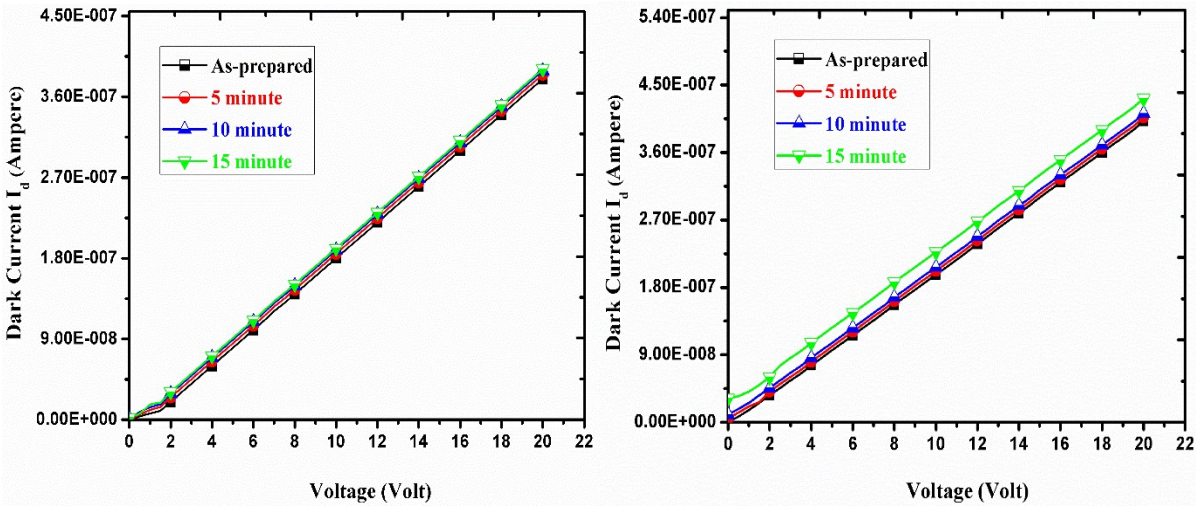

Figure.10. Variation of dark current with voltage of as-prepared and laser irradiated, thin films of (a) $Se_{90}S_{10}$, and (b) $Se_{75}Hg_{15}S_{10}$.

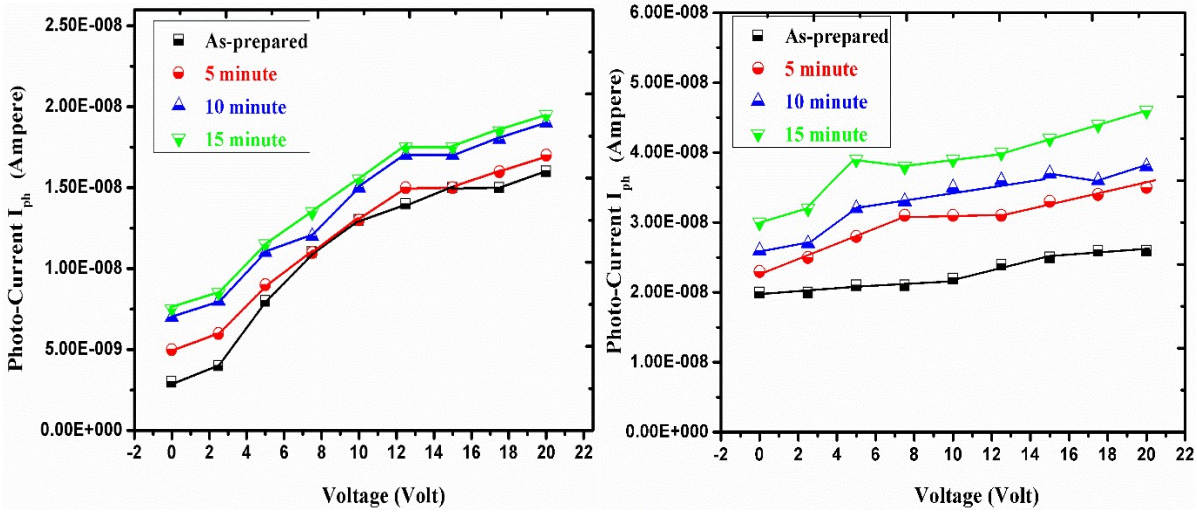

Figure.11. Variation of photocurrent with voltage of as-prepared and laser irradiated, thin films of (a) $Se_{90}S_{10}$, and (b) $Se_{75}Hg_{15}S_{10}$.

The dark conductivity of chalcogenide semiconductor generally depends on density and mobility of charge carriers. In this study the dc conductivity (σ_{dc}) was estimated in the temperature range of 307.5-391.9 K at constant voltage of 1.5 V. Fig.12 displays temperature dependent dc conductivity (σ_{dc}) of as-prepared and laser irradiated thin films of $Se_{90-x}Hg_xS_{10}$ (x = 0, 5, 10, 15).

Plots of ln σ_{dc} versus 1000/T are found to be straight lines which indicate the conduction is through an activated process and obeys Arrhenius relation [38] as

$$\sigma_{dc} = \sigma_0 \exp[-\Delta E_{dc}/KT] \quad (6)$$

where σ_0 is pre-exponential factor related to the material, ΔE_{dc} is activation energy and K is the Boltzmann constant and T is temperature. The values of activation energy (ΔE_{dc}) are calculated from the slope of ln σ_{dc} versus 1000/T and using Eq. (6). The slope of the curve is estimated by using linear fit. The calculated values of activation energy (ΔE_{dc}), dcconductivity (σ_{dc}) and pre-exponential factor (σ_0) are given in Table.1. It is clearly found that the dc conductivity increases and the corresponding activation energy decreases with irradiation time as shown in Fig.12. There is variation of steady state photoconductivity (σ_{ph}) of investigated thin films with temperature at intensity (3650 lx). The ΔE_{ph} is estimated by the slope of Fig.13 and its values follows the same trend as that of ΔE_{dc} as shown in Table.1. Both dark dc conductivity and photoconductivity increase exponentially with temperature and this imply that conduction is through thermally activated process. Further the conduction in amorphous semiconductors can occur in three different ways [38]

(i) At low temperature, the conduction is due to thermally assisted tunneling between the states at Fermi-level.
(ii) At intermediate temperature, the conduction is due to the excitation of charge carriers into the localized states of the band tails, the carriers can take place in transport by hopping in these localized states.
(iii) At higher temperature, carriers are excited into the extended states.

According to Davis Mott model [38], the value of pre-exponential factor (σ_0), also called Mott parameter, decides the electrical conduction mechanism of amorphous semiconductors. The value of pre-exponential factor (σ_0) for extended state conduction lies in the range of 10^3-10^4S cm^{-1}, and for hopping conduction in localized states, the value of σ_0 is very small. In the present case, the value of σ_0 is very small (10^0-10^{-2}S cm^{-1}) so the conduction of the investigated thin films is due to hopping in localized states. The temperature dependent steady state photoconductivity curve in amorphous semiconductors shows three regimes [38-40]:

(i) At low temperature, the photoconductivity is directly proportional to the generation rate 'g' and remains nearly constant with temperature.
(ii) At intermediate temperature, the photoconductivity increases with temperature by several orders of magnitude. In this regime, the rate of recombination is governed by the photo-generated carriers and the photoconductivity is directly proportional to the g^{γ} and is less than dark d.c. conductivity.
(iii) At higher temperature the photoconductivity decreases with temperature and is proportional to the intensity.

The present study of temperature dependent photoconductivity follows the second regime as measurements have been taken in intermediate range. From Fig.14, it has been found that photosensitivity (σ_{ph}/σ_{dc}) of the investigated thin films remains nearly constant up to 10 min of laser irradiation and after 15 min, it increases with laser irradiation for all compositions of $Se_{90-x}Hg_xS_{10}$.

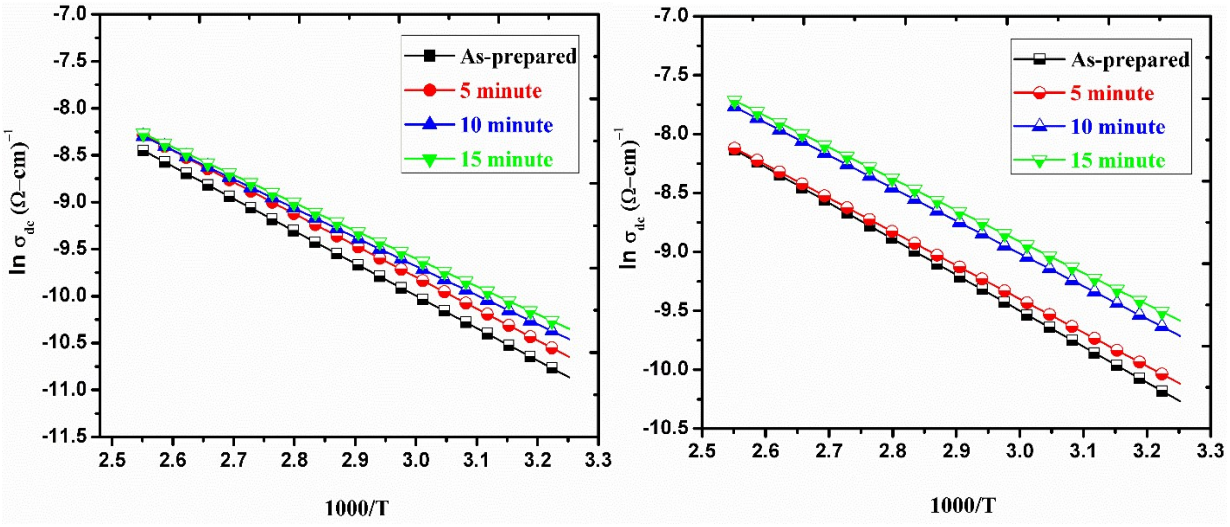

Figure.12. Variation of dark d. c. conductivity (σ_{dc}) with 1000/T of as-prepared and laser irradiated, thin films of (a) $Se_{90}S_{10}$, and (b) $Se_{75}Hg_{15}S_{10}$.

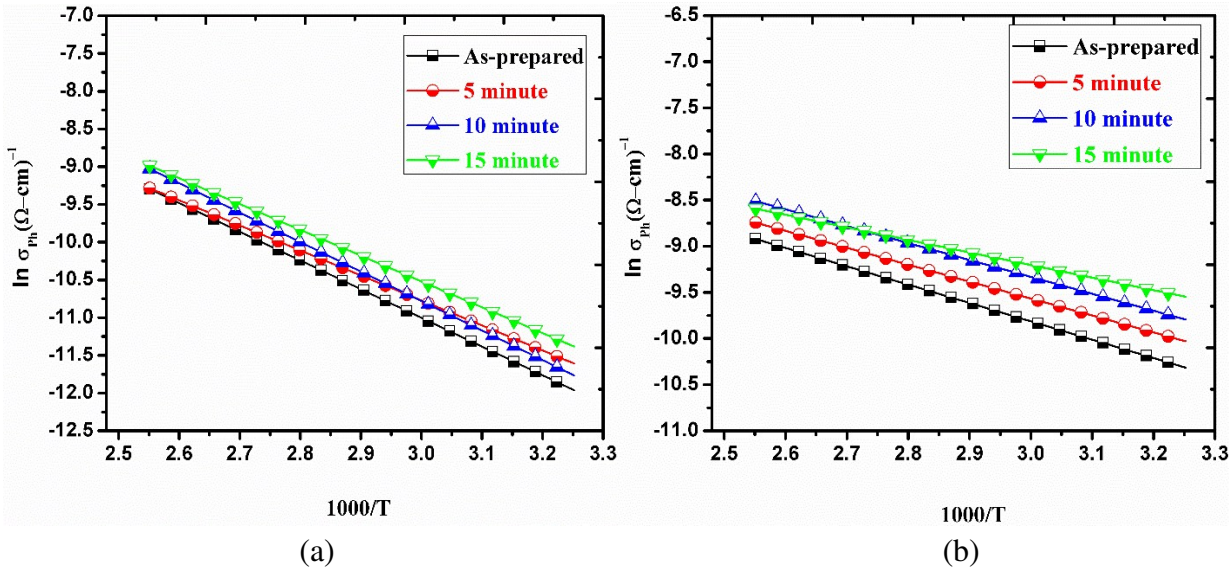

Figure.13. Variation of photo-conductivity (σ_{ph}) with 1000/T of as-prepared and laser irradiated, thin films of (a) $Se_{90}S_{10}$, and (b) $Se_{75}Hg_{15}S_{10}$.

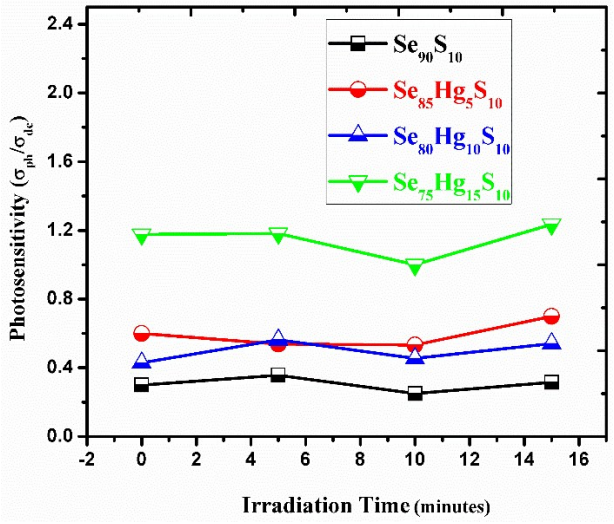

Figure.14. Variation of photosensitivty with irradiation time of as-prepared and laser irradiated, thin films of $Se_{90-x}Hg_xS_{10}$ (x = 0,5, 10, 15) at room temperature.

4. **Discussion**

Above results show the modification of structural, optical and electrical properties of amorphous $Se_{90-x}Hg_xS_{10}$ (x = 0,5, 10, 15) thin films by laser irradiation. Both structural and surface morphological analysis revealed the transition from amorphous to crystalline phase after irradiation. However, due to the amorphous natuure of as-prepared thin films, there are dense defect states present in between the forbidden energy gap also known as 'Urbachs energy band' whose density varies exponentially as one moves from valence band to conduction band edges. These defect states are annealed out after laser irradiation as confirmed by Urbach's energy (see Table.1) whose value decreases with irradiation for all compositions. The optical analysis also shows the reduction in optical band gap with irradiation (see Table.1). This reduction of optical band gap was interpreted in terms of increase of grain size, because it is one of the important factors which could affect the optical band. If the grain size increases to a few nm the optical band gap should decrease[41], which holds good in the present study. Previous studies also showed the similar kind of trend between the optical band gap and grain sizes [31, 42, 43]. The values of absorption coefficient increased with irradiation for all compositions of $Se_{90-x}Hg_xS_{10}$ which lies in the range of $10^{-4}cm^{-1}$ before and after irradiation. The significant imprvement was found in both dark curent and photo-current (see Fig.10, 11) after laser irradiation. This remarkable change is explained on the basis of dense defect states present near the valence and coduction bands of the as-prepared thin films.The defect states will trap the charge carriers and reduces the mobility range, and hence the current. However, after irradiation these defects states are annealed out, and the current in these films increases. Similar trends are also observed in the case of temperature dependent dark dc conductivity and photoconductivity measurements (see Fig.12, 13). This significant improvement in the values of absorption coefficient, d. c conductivity and photoconductivity and photosensitivity makes these material suitable for many

optoelectronic devices. For example for solar cell applications the optimum band of the material is 1.5 eV for producing maximum efficiency. This study shows the value of optical band gap of Se-S reaches to 1.66 eV (shown in table 1.d) after the addition of 15 % of Hg and after 15 min laser irradiation, which is very close to the optimum band gap. Thus $Se_{75}Hg_{15}S_{10}$ is good material for solar cell applications. Smilarly the other compositions have also useful in other optoelectronic device applications.

5. Conclusion

Present study demonstrates that the thin films of $Se_{90-x}Hg_xS_{10}$ undergo amorphous to crystalline phase when irradiated with laser. This structural transformation has been analyzed by XRD, SEM and AFM. Surface morphological analysis revealed the the value of grain size increases after laser irradiation. The surface morphology results analyzed by AFM favours this enhancement of grain size after laser irradiation. Optical analysis shows the decrease of optical band gap of $Se_{90-x}Hg_xS_{10}$ (x = 0,5, 10, 15) after irradiation and the corresponding absorption coefficient increases with laser irrdiation. Electrical analysis displays the dark dc conductivity and photoconductivity enhances with laser irradiation. It was also found that the value of activation energy decreases after irrdiation. Such significant improvement in the values of absorption coefficient, optical band gap, photoconductivity etc. makes these materials suitable for many optoelectronic device applications.

Acknowledgement

Authors (S.A, M.Z) are very thankful to the Department of Physics, Jamia Millia Islamia, New Delhi, India, for their support in this work and encouragement and also to Mrs. Indra Sulania, IUAC New Delhi, India, for providing us AFM measurement facility in this research. The Author, S. A, is thankful to University Grants Commission (UGC) for the financial assistance.

References

[1] N. Yamada, Materials Research Society Bulletin, 21 (1996) 48.
[2] A.A. Al-Ghamdi, Shamshad A. Khan, S. Al-Heniti, F.A. Al-Agel, M. Zulfequar, Current Applied Physics 11 (2011) 315-320,
[3] Y. Raviprakash, Kasturi V. Bangera, G.K. Shivakumar, Curr. Appl. Phys.10 (2010) 193.
[4] Muneer Ahmad, J. Kumar, R. Thangaraj, J. Non-Cryst. Solids 355 (2009) 2345.
[5] A. Ganjoo, K. Shimakawa, H. Kamiya, E.A. Davis, Jai Singh, Phys. Rev. B 62 /2000) 14601
[6] Vladimir V. Poborchii, Alexander V. Kolobov, Kazunobu Tanaka, Appl. Phys. Lett. 74 (1999) 215.
[7] Gang Chen, Himanshu Jain, Syed Khalid, Jun Li, David A. Drabold, Stephen R. Elliott, Solid State Communications 120 /2001) 149-153.
[8] K. Takana, Phys. Rev. B 57 (1998) 5163.
[9] F.A. Al-Agel, Vacuum 85 (2011) 892-897

[10] N. A. Hegab, H.M. El-Mallah,ACTA PHYSICA POLONICA A Vol. 118 (2010) 637-642
[11] Shanshan Song, Nathan Carlie, Julie Boudies, Laeticia Petit, Kathleen Richardson, Craig B. Arnold, Journal of Non-Crystalline Solids 355 (2009) 2272–2278,
[12] Shabir Ahmad, Mohsin Ganaie, Mohd. Shahid Khan, K. Asokan and M. Zulfequar, Radiation Effects & Defects in Solids, 170, (2015) 30–42.
[13] Victor I Mikla, Victor V. Mikla, Amorphous Chalcogenides, 2012, ISBN: 978-0-12-388429-9, p-1.
[14].S. Diamond, David S. Weiss, Hand Book of Imaging Materials, Second edition, Chapter.9, (2002) p-329, ISBN: 0-8247-8903-2,
[15] Jaques I. Pankove, Hydrogenated Amorphous Silicon, (1984), Academic press, INC, p- 1, ISBN: 0-12- 752150- x, Vol. 21, p- 75, chapter 5.
[16] Suzanne Easton, Practical VerterinaryDignostic Imaging, Second edition, chapter 12, 2012, ISBN: 978-0-470-65648-8
[17]S. Abbaszadeh, K.S. Karim, V. Karanassios, IEEE Trans. Electr. (2013), 60, 880–883.
[18]S. Kasap, J.B. Frey, G. Belev, O. Tousignant, H. Mani, J. Greenspan, L. Laperriere, O. Bubon, A. Reznik, G. DeCrescenzo, Sensors 2011, 11, 5112–5157.
[19] S.O. Kasap, J.A. Rowlands, IEEE Proc. Cirt. Dev. Syst. 2002, 149, 85–96.
[20] Mohd. Nasir, M. Zulfequar, Journal of Physics and Chemistry of Solids, 74 (2013) 1527-1532.
[21] Mohsin Ganaie, M. Zulfequar, Journal of Materials Science: Materials in Electronics, DOI: 10.1007/s10854-015-4118-5.
[22] M. Abkowitz, Polymer Eng.Sci., 24 (14) (1984) 1149-1154.
[23] M. A. Alvi, Current Applied Physics, 13 (2013) 474-478
[24] F. A. Al-Agel, E. A. Al-Arfaz, F. M. Al-Marzouki, Shamshad A. Khan, Zishan H. Khan, A.A. Al-Ghamdi, Material Science in Semiconductor Processing 16 (2013) 884-892.
[25] Maissel, L.I;Glang, R. Handbook of Thin Film Technology; McGraw-Hill: New York, 1980.
[26] D.P. Gosain, T. Shimizu, M. Ohmura, M. Suzuki, T. Bando, S. Okano, J. Mater. Sci.26 (1991) 3271.
[27] Shabir Ahmad, K. Asokanand M. Zulfequar, Philosophical Magazine, Vol. 95, No. 12 (2015) 1309–1320.
[28] J. Tauc, Amorphous and liquid semiconductors, (New York: Plenum Press, 171 (1974).
[29] F. Urbach, Phys. Rev. 92 (1953) 1324
[30]E. A. David and N. F. Mott, Philos. Mag.22 (1970) 903.
[31] M.R. Balboul, Radiation Measurements 43 (2008) 1360.
[32] G. Saffarini, J.M. Saiter, H. Schmitt, Optical Materials 29 (2007) 1143.
[33] F.A. Al-Agel, E.A. Al-Arfaj , F.M. Al-Marzouki , Shamshad A. Khan, A.A. Al-Ghamdi, Progress in Natural Science: Materials International 23 (2) (2013) 139–144.
[34] Shabir Ahmad, K. Asokan, Mohd. Shahid Khan and M. Zulfequar, Philosophical Magazine, Vol. 95, No. 22 (2015) 2385–2402.

[35] Jiang Wu, Zhiming M. Wang, Quantum Dot Solar Cells, Springer New York Heidilberg Dordrecht London, 2014, ISBN: 978-1-4614-8147-8.Chapter 2, Page42.
[36] H. Kurisu, T. Tanaka, T. Karasawa and T. Komatsu, Jpn. J. Appl. Phys. 32 (1993): 285–287.
[37] Lee.Chieh-Ju, Mizel. Ari, Banin. Uri, L. Cohen. Marvin, Alivisatos, A. Paul, The Journal of Chemical Physics, 5 (2000) 113.
[38] N. F. Mott, E. A. Davis (Eds), Non-Crystalline Materials, Clarendon, Oxford, 1979
[39] J. M. Marshall, C. Main, E. E. Owen, J. Non-Crystalline Solids, 8 (1972) 760
[40] P. G. LeComber, J. Mort (Eds), Electronic and structural Properties of Semiconductors, Academic, London and New York, 1973.
[41] R. Sreekumar, R. Jayakrishan, C. Sudha Kartha, K.P. Vijay Kumar, S. A. Khan, D. K. Avasthi, J. App. Phys. 103 (2008) 023709.
[42] N. Choudhury, F. Singh, B. K. Sarma, Indian Journal of Pure and Applied Physics, 50 (2012) 325-328.
[43] Ausama I. Khudiar, M. Zulfequar and Zahid H. Khan, Radiation Effects & Defects in Solids, 2009, Vol. 164, No. 9, 551–560.